FRACTURE OF CONCRETE AND ROCK

SEM-RILEM International Conference

June 17-19, 1987

Houston, TX, USA

Editors

Surendra P. Shah

Northwestern University
Evanston, IL, USA

Stuart E. Swartz

Kansas State University
Manhattan, KS, USA

SEM/RILEM International Conference
on Fracture of Concrete and Rock
Houston, Texas, June 1987
Editors: S.P. Shah, S.E. Swartz

FRACTURE ENERGY OF HETEROGENEOUS MATERIALS AND SIMILITUDE

Zdeněk P. Bažant*

ABSTRACT

The paper reviews the size effect accompanying blunt fracture in brittle heterogeneous materials such as concrete and its applications to structural analysis and design. Various refinements of Bažant's size effect law are summarized, and recent results of fracture tests of Bazant and Pfeiffer which establish measurements of concrete fracture energy on the basis of size effect are given. These test results confirm that fracture energy may be uniquely defined by size extrapolation to infinity. Furthermore, changes in the size effect caused by temperature and humidity are considered, a new formula for the effect of temperature on fracture energy is derived on the basis of the activation energy concept, and some of the test results of Prat and Bazant which determine the temperature and humidity effect on fracture energy are given. Finally, similitude of brittle failures due to blunt fracture is analyzed in three dimensions and it is shown that the same form of the size effect law as for two dimensions is applicable.

INTRODUCTION

The size effect, which consists in the fact that the nominal stress at failure of geometrically similar structures of different sizes is not constant but decreases with the size, is no doubt the most important aspect of fracture mechanics, setting it apart from stress-based failure theories such as plasticity. The present paper will review various recent advances in this subject and focus particular attention on the use of the size effect for determining the fracture energy, as well as the changes in the size effect brought about by changes of temperature, and their consequence for the dependence of fracture energy on temperature. A generalization of the size effect law to three dimensions will be also studied.

SIZE EFFECT LAW AND ITS REFINEMENTS

The size effect may be isolated from other influences by considering geometrically similar structures of different sizes. For fractures blunted by distributed cracking, the simplest description of the size effect is provided by the approximate size effect law [1] (Fig. 1):

$$\sigma_N = Bf'_t\left(1 + \frac{d}{\lambda_0 d_a}\right)^{-1/2} \qquad (1)$$

in which σ_N is the nominal stress at failure (the failure load divided by the characteristic dimension and structure thickness), d is the characteristic dimension of the structure, d_a is the maximum size of material inhomogeneities, e.g., the aggregate size in concrete; f'_t = tensile stength (from direct tensile tests), and B, λ_0 = empirical constants. The size effect law has been shown to follow by dimensional analysis and similitude arguments from the following two simplifying hypotheses:

1. The energy release W due to failure is a function of the length a of the fracture.

2. At the same time, W is a function of the volume of the zone of cracking or, alternatively, of the size of the fracture process zone at fracture front.

The second hypothesis alone leads to plastic limit analysis, which exhibits no size effect, and the first hypothesis alone leads to classical linear elastic fracture mechanics, which exhibits the strongest possible size effect. We deal with the type of failure which requires a combination of both.

Eq. (1) represents the simplest possible formula for the transition between failures dominated by the strength limit and failures dominated by energy dissipation at fracture front and characterized by fracture

*Professor of Civil Engineering, Northwestern University, Evanston, Illinois 60201.

energy. It has been shown that Eq. (1) correctly describes the results of fracture tests of concrete within the scatter range of measurements [5], and that it can also be applied to the failure of various concrete structures which fail in a brittle manner. These include the diagonal shear failure of prestressed and unprestressed reinforced concrete beams without stirrups, the torsional failures of concrete beams, the beam and ring failures of unreinforced pipes, the punching shear failure of reinforced concrete slabs, etc. In making these applications, two further hypotheses are implied in the use of the size effect law in Eq. (1):

1. The shapes of the final fractures at failure in specimens of different sizes are geometrically similar; and

2. The failure does not occur at crack initiation.

The latter hypothesis is practically always satisfied since it is prohibited by codes to design concrete structures which would fail at the first crack initiation. The approximate applicability of the first hypothesis appears to be verified by the existing test data.

The scatter of existing measurements is not sufficiently small to make it possible to detect significant deviations from the size effect law in Eq. (1). However, finite element computations can be carried out to make comparisons with the size effect law [3,4]. One such calculation has recently been carried out by Hillerborg [4] using his fictitious crack model for a three-point bent fracture test. Considering specimen size range of the ratio 1:250 (which is much broader than one can realize in practice, due to cost limitations), he detected appreciable deviations from Eq. 1; see the results in Table 1.

TABLE 1. Comparison of size effect law (with r=0.44, B=306, λ_0=0.608) and Hillerborg's finite element results with fictitious crack model

$df_t'^2/EG_f$	σ_N/f_t'	
	Finite Elements (Hillerborg)	Size Effect Law
0.02	2.43	2.44
0.05	2.22	2.21
0.1	2.01	2.00
0.2	1.77	1.78
0.5	1.46	1.46
1	1.222	1.222
2	0.992	0.995
5	0.725	0.739

It has been shown, however, [3], that a refinement of the size effect law is possible such that it closely agrees with Hillerborg's finite element results; see the last column in Table 1 which is so close to Hillerborg's results that a graphical distinction is hardly possible. These results are based on the following generalized size effect law [2,20]:

$$\sigma_N = Bf_t^*\left[1 + \left(\frac{d}{\lambda_0 d_a}\right)^r\right]^{-1/2r} \tag{2}$$

which itself is a special case of the general asymptotic series expansion [2]:

$$\sigma_N = Bf_t^*(c_0\xi^{-1} + 1 + c_1\xi + c_2\xi^2 + c_3\xi^3 + \ldots)^{-1/2r}, \quad \xi = \left(\frac{d_a}{d}\right)^r \tag{3}$$

in which $f_t^* = f_t'$ if the aggregate size d_a is the same for all specimens, and B, λ_0, r are empirical parameters, and so are the coefficients c_0, c_1, c_2,... If the aggregate size d_a is varied, then theoretical analysis leads to the formula [5]:

$$f_t^* = f_t'\left[1 + \left(\frac{c_0}{d_a}\right)^{1/2}\right] \tag{4}$$

which is similar to the Petch formula [6,7,8] for the effect of grain size on the yield limit of polycrystalline metals.

It has been established [8] that there is a one-two-one relationship between the size effect law and the shape of the softening portion of the stress-displacement diagram used in Hillerborg's type models. When one of these relations is known, the other one can be determined. The same is true for the crack band model, in which the front of the strain-softening damage is assumed to have a certain constant width which is a material property; to each shape of the strain-softening stress-strain diagram there corresponds a certain size effect law and vice versa. No doubt this is also true of the damage laws. Furthermore, if the front of the band of strain-softening damage is variable, this has a direct effect on the size effect law, and from size effect observations it is possible to make inferences on the size of the strain-softening zone.

A similar one-to-one relationship was previously established between the size effect law and the R-curves from blunt fracture tests [8].

The size effect is of interest not only with regard to fracture testing and design of structures. The size effect is equaly valuable for checking the soundness of finite element models. At present, models of cracking which are formulated strictly on the basis of stress-strain relations and pay no attention to strain-localization instabilities and energy aspects of failure are still in prevalent use. All these finite element codes predict the nominal stress at failure for structures of different sizes which are geometrically similar and are analyzed with geometrically similar meshes to be the same. Experimental evidence clearly indicates that for brittle failures such predictions are incorrect. This may be one reason that despite two decades of effort, the existing finite element codes still cannot reliably predict brittle failures of concrete structures, except perhaps when the parameters of the model are calibrated for one structure size and predictions are made for roughly the same size.

A check for the size effect, and comparisons with the theoretically derived size effect law or experimental evidence, if available, should be an integral part of evaluation of the applicability of every finite element code to brittle failures due to cracking of concrete as well as rock.

DEFINITION AND DETERMINATION OF FRACTURE ENERGY ON THE BASIS OF SIZE EFFECT

The size effect observed on geometrically similar specimens appears as the best means for identifying the material properties which govern fracture. The most important among these properties is the fracture energy. The fracture energy of materials such as concrete has proven difficult to determine as well as define. Various testing methods currently in use yield results which may differ by several hundred percent, and aside from that, none of the existing definitions of the fracture energy appears to yield unique results.

Based on the size effect, it now appears that a unique definition of fracture energy can be provided as follows [2,9]:

The fracture energy G_f of a heterogeneous brittle material is the specific energy required for fracture propagation in a geometrically similar specimen of infinite size.

It has been shown [2,8] that this definition leads to the formula:

$$G_f = \frac{g_F}{A E_c} f_t'^2 d_a = \frac{g_F}{E_c} B^2 \lambda_0 f_t'^2 d_a \qquad (5)$$

in which B, λ_0, d_a are the parameters of the size effect law, E_c is the elastic modulus of the material, A = slope of the regression line in Fig. 1, and g_F is the nondimensional energy release rate for a sharp fracture, calculated according to linear elastic fracture mechanics. It can be theoretically shown that the fracture energy for specimen size extrapolated to infinity must be the same for all specimen shapes [9]. Indeed, for an infinitely large specimen, the relative size of the strain-softening damage zone is infinitely small, and the zone is surrounded by the asymptotic elastic field known from linear elastic fracture mechanics, which is the same regardless of the structure geometry. Therefore, at extrapolation to infinity, the detailed picture of the fracture process zone must be the same for all structure geometries.

This theoretical conclusion has been verified experimentally [9]. Specimens made of the same concrete were cast in different sizes, and different types of notches as well as different types of loading were used. The test series included three point bent specimens, centrically tensioned edge-notched specimens, and eccentrically compressed specimens (Fig. 1). These shapes include just about the extreme of the range of conditions to which the ligament cross section may be exposed: bending moment over the ligament, tensile force over the ligament, and a combination of bending moment and force over the ligament.

The results of these tests conducted at Northwestern University are exhibited in Fig. 1 in terms of the plots of σ_N^{-2} versus d/d_a. According to the size effect law, these plots should ideally be straight lines, which makes it possible to use linear regression for the determination of the parameters of the size effect law. The slope of the regression line is proportional to the inverse of the fracture energy, in view of Eq. (5). Based on slopes of the regression lines of the test results in Fig. 1, it is found that the fracture energy for the three types of specimens are about the same, and do not deviate from each other more than is inevitable for a heterogeneous material such as concrete (the deviations from the mean are within ± 3%); see Table 2.

TABLE 2. Fracture Energy Values Obtained from Measurements Evaluated by Size Effect Law (lb./in.)

Specimen Type	Concrete	Mortar
1) Three-Point Bent	0.229	0.129
2) Edge-Notched Tension	0.210	0.118
3) Eccentric Compression	0.233	0.132

Noting at the same time that, by definition, this method of determining fracture energy is independent of the specimen size, it appears that the determination of fracture energy on the basis of the size effect indeed yields unique results. This cannot be said of other existing methods.

The size effect law in Eq. (1) is nevertheless an approximation, and deviations occur when a broad range of sizes is considered or accurate results are desired. Important work in this direction has been recently carried out by Planas and Elices at Technical University in Madrid (private communication, 1986). They considered various strain-softening formulations and calculated the corresponding size effect curves for certain types of specimens using the Green's function approach. By matching such curves to test results it should be possible, in principle, to gain further information on the material parameters that govern strain-softening.

SIZE EFFECT IN THREE DIMENSIONS

The size effect due to blunt fracture has so far been treated in a two-dimensional context, assuming the state of plane stress or plane strain and uniform conditions throughout the thickness. In two experimental studies [9,10], however, the size effect law (Eq. 1) was used for brittle three-dimensional failures -- the punching shear failure of circular reinforced concrete slabs and the torsional failure of unreinforced or longitudinally reinforced concrete beams. In the course of these studies it was experimentally verified that Eq. 1 can be extended to three-dimensions, and the theoretical proof will be presented now.

The two fundamental similifying hypotheses listed under Eq. 1 remain applicable in three-dimensions. Similar to the previous derivation [1,2], these fundamental hypotheses mean that the failure is describable in terms of two parameters, a and $k_0 a^2 n d_a$, the latter one representing the volume of the cracking zone (Fig. 2). Coefficient k_0 characterizes the geometry of the failure zone and is constant if geometrically similar bodies with geometrically similar failure modes are considered; d_a = maximum aggregate size (or more generally inhomogeneity size), and n = empirical coefficient, for concrete typically about n = 3, such that nd_a represents the effective width of the front of cracking or alternatively the length of the fracture process zone (these two meanings were shown to lead to the same result; see Ref. 21). The foregoing two parameters, however, are not nondimensional. It must, of course, be possible to describe the failure in terms of nondimensional parameters, and for this purpose length a must be divided by a quantity of the dimension of length, and volume $k_0 a\, nd_a$ by a quantity of the dimension of volume. We choose to divide these two parameters by d and $k_0 a^2 d$, respectively (other choices are equally possible and yield the same result, but the derivation is the simplest for this choice). Thus, the nondimensional parameters for our problems are:

$$\theta_1 = \frac{a}{d}\,, \qquad \theta_2 = \frac{k_0\, a^2\, nd_a}{k_0\, a^2\, d} = \frac{nd_a}{d} \tag{6}$$

Parameter θ_1 represents the relative size of the fracture, and parameter θ_2 the relative volume of the cracking zone. Fig. 2a shows an example of three-dimensional fracture which is axisymmetric, but the foregoing description holds for arbitrary three-dimensional geometries provided there is geometrical similarity between various sizes; see Fig. 2b.

We now consider geometrically similar specimens or structures of different sizes d (Fig. 2b), characterized by a constant ratio a/d. Thus, parameter θ_1 is size-independent, while parameter θ_2 characterizes the size. As in the previous studies [1,2], the total release of potential energy W from the structure may always be given in the form:

$$W = \left[\frac{1}{2E_c}\left(\frac{P}{d^2}\right)^2\right] d^3\, F(\theta_1, \theta_2) = \frac{P^2}{2E_c}\,\frac{F(\theta_1, \theta_2)}{d} \tag{7}$$

in which E_c is the Young's elastic modulus of concrete, P is the maximum load (i.e., the failure load under load-controlled conditions), and F is a certain function of the nondimensional parameters, characteristic of the given geometry of the structure and the cracking zone. The essential point is that function F must be the same for different sizes if the structures or specimens are geometrically similar. Energy balance during failure requires that:

$$\left[\frac{\partial W}{\partial a}\right]_{d\,=\,\text{const.}} = kd\, G_f \tag{8}$$

in which kd represents the length of the perimeter of the fracture front, k being an empirical coefficient independent of size d, and G_f is the fracture energy of the material. Differentiating Eq. 7 with respect to a and substituting into Eq. 8, we have:

$$\frac{P^2}{2E_c d}\,\frac{\partial F}{\partial \theta_1}\,\frac{1}{d} = k\, d\, G_f \tag{9}$$

The nominal stress at failure may be defined in three-dimensions as $\sigma_N = P/d^2$, and so we get:

$$\sigma_N = \frac{P}{d^2} = \left(\frac{2k\ G_b\ E_c}{(\partial F/\partial\theta_1)\ d}\right)^{1/2} \tag{10}$$

The state $\theta_2 = 0$, which corresponds to an infinitely large structure ($d/d_a \to \infty$) may now be chosen as the reference state, and $\partial F/\partial\theta_1$ may be expanded as a function of θ_2 in Taylor series:

$$\frac{\partial F(\theta_1, \theta_2)}{\partial\theta_1} = f_0(\theta_1) + f_1(\theta_1)\ \theta_2 + f_2(\theta_1)\ \theta_2^2 + f_3(\theta_1)\ \theta_2^3 + \ldots \tag{11}$$

in which we introduce the notations:

$$f_1(\theta_1) = \frac{1}{1!}\left[\frac{\partial F}{\partial\theta_2}\right]_{\theta_2 = 0}, \quad f_2(\theta_1) = \frac{1}{2!}\left[\frac{\partial^2 F}{\partial\theta_2^2}\right]_{\theta_2 = 0}, \quad f_3(\theta_1) = \frac{1}{3!}\left[\frac{\partial^3 F}{\partial\theta_2^3}\right]_{\theta_2 = 0}, \tag{12}$$

Substitution of Eq. 11 into Eq. 10 then yields for the size effect the asymptotic expansion:

$$\sigma_N = Bf_t'\left[1 + \frac{d}{\lambda_0 d_a} + \lambda_1\frac{d_a}{d} + \lambda_2\left(\frac{d_a}{d}\right)^2 + \lambda_3\left(\frac{d_a}{d}\right)^3 + \ldots\right]^{-1/2} \tag{13}$$

in which we introduced the following constants:

$$B = \frac{2k}{f_1\, nd_a}\frac{(G_f\ E_c)^{-1/2}}{f_t'}, \quad \lambda_0 = \frac{f_1}{f_2}, \quad \lambda_1 = \frac{f_2}{f_1}, \quad \lambda_3 = \frac{f_3}{f_1}, \ \ldots \tag{14}$$

and f_t' denotes the direct tensile strength of the material. The constants in Eq. 14 depend on the geometry of the structure and of the cracking zone.

If we adopt the viewpoint of a cracking band of effective width nd_a at the cracking front, we may express the fracture energy as:

$$G_f = nd_a\frac{f_t'^2}{2}\left(\frac{1}{E_c} - \frac{1}{E_t}\right) \tag{15}$$

in which E_t denotes the mean softening modulus, i.e., the mean slope of the descending branch of the stress-strain diagram. Then the expression for B becomes

$$B = \left[\frac{k}{f_1}\left(1 - \frac{E_c}{E_t}\right)\right]^{1/2} \tag{15a}$$

Eq. 13, which is of the same form as derived before for two dimensions (Ref. 2, Eq. 39), describes the most general possible size effect. The first-degree approximation is obtained by deleting the terms with coefficients $\lambda_1, \lambda_2, \ldots$, and this yields Eq. 1 stated at the outset and originally derived for two-dimensions.

It may be noted that the function which is expanded into the asymptotic series in Eq. 11 could be chosen as $(\partial F/\partial\theta_1)^r$ instead of $\partial F/\partial\theta_1$. In that case, one obtains in the same manner a still more general expression for the size effect:

$$\sigma_N = Bf_t'\left(c_0\xi^{-1} + 1 + c_2\xi + c_3\xi^2 + c_4\xi^3 + \ldots\right)^{-1/2r}, \quad \xi = (d/d_a)^r \tag{16}$$

in which $c_0, c_2, c_3 \ldots$ are certain constants. This expansion makes it possible to describe the size effect over a broader range with fewer terms, as illustrated in the example of Table 1. However, it is not clear whether Eq. 16 for $r = 1$ yields the correct initial asymptotic behavior for a very small size ($d \to 0$).

The idea that the approximate size effect law should be of general applicability was initially conceived [1] upon noting that calculations for various specific geometries yield the same result. Let us now carry out a similar calculation, choosing as an example the axisymmetric specimen in Fig. 2a with a cylindrical cracking

zone 123456 of diameter a (Fig. 2a). Before cracking, the specimen is under uniform uniaxial stress σ_N, with resultant $P = \sigma_N d^2/4$ where d is chosen to represent the diameter of the specimen. The energy release may be considered to approximately equal the strain energy initially contained within the cracking layer (cylinder 123456) and in cones 1237 and 4568 (Fig. 2a) adjacent to this layer. The height of these cones is considered as $k_1 a$, k_1 being an empirical constant, imagined to represent the slope of the "stress diffusion" lines, represented here by the slope of the cone. The stress diffusion concept is of course approximate, however, it yields dimensionally correct results, and this is all that matters for our purpose. The total energy release may thus be expressed as:

$$W = \left(2\,\frac{k_1 a}{3}\,\frac{\pi a^2}{4} + n d_a\,\frac{\pi a^2}{4}\right)\frac{\sigma_N^2}{2E_c} \tag{17}$$

Eq. 8 for energy balance now takes the form:

$$\partial W/\partial a = \pi\, a\, G_f \tag{18}$$

Substituting for G_f Eq. 15, evaluating the derivative of Eq. 17 with respect to a, and solving for σ_N, we now get again Eq. 1 in which:

$$B = \sqrt{2}\left(1 - \frac{E}{E_t}\right)^{1/2}, \qquad \lambda_0 = \frac{n\, d_a}{k_1}\,\frac{d}{a} \tag{19}$$

So the result agrees with the first order approximation according to Eq. 13. A similar agreement can be demonstrated for various other simple geometries such as edge-cracked cylinder, or square prism with a square crack layer, etc.

SIMILITUDE OF FRACTURE RATES AND DEPENDENCE OF FRACTURE ENERGY ON TEMPERATURE

It is generally assumed that the fracture energy of concrete depends on temperature, but no formula is apparently available. While heating causes in metals abrupt increases of fracture toughness, due to brittle-ductile transitions which change the fracture mechanism, the fracture toughness of purely brittle materials, such as glass, ceramics, graphite and rocks is known to smoothly decrease with increasing temperature [11,12,13]. We will now show the derivation of a simple formula, exploiting the similitude of fracture rates at various temperatures. This is, of course, a completely different type of similitude than that which governs the size effect.

It is generally accepted that fracture is a thermally activated rate process. This means that the atomic bond ruptures which constitute the mechanism of fracture are provoked by the energies of thermal vibrations [14]. These energies are statistically distributed, which is known to be described by the Maxwell distribution, and a rise of temperature causes an increase of the probability (or frequency) that the atom's energy would exceed the activation energy barrier of the bond. Therefore, a rise of temperature produces an increase in the growth rate of fracture, which generally follows a formula of the type [15]:

$$\dot{a} = \phi(K)\, e^{-U/RT} \tag{20}$$

in which $\dot{a}$ = rate of growth of fracture length, U = activation energy of bond rupture, R = universal gas constant, T = absolute temperature, K = stress intensity factor, and $\phi(K)$ = an empirical function, increasing monotonically.

Recently, Evans [16,17] and Thouless et al. [18] proposed and verified for ceramics a special form of Eq. 20:

$$\dot{a} = v_c\left(\frac{K}{K_c}\right)^n e^{-U/RT} \tag{21}$$

where K_c = critical value of fracture toughness, and v_c, n = empirical constants characterizing the given material.

A formula of this type may be expected to apply also for concrete. Eq. 21 is not exact but only approximate, for two reasons: 1) the proportionality of $\dot{a}$ to K^n is only empirical, and 2) more than one mechanism of atomic bond rupture, with different activation energies, might be involved, and the type of fracture mechanism might change with temperature.

Because of the well-known relations $K = (GE_c)^{1/2}$ and $K_c = (G_f^0 E_c)^{1/2}$, where G = rate of energy release

from the structure into the fracture process zone [19,20], Eq. 21 may be rewritten as:

$$\dot{a} = v_c\left(\frac{G}{G_f}\right)^{n/2}\left[\exp - \frac{U}{R}\left(\frac{1}{T} - \frac{1}{T_0}\right)\right] \tag{22}$$

Eq. 22 may serve as the basic relation for determining the crack growth in time. Although the time-dependent fracture description in terms of the crack growth rate is no doubt physically more fundamental, the time-independent fracture description prevails in applications. In fact, what is known as fracture mechanics is a time-independent theory. So we need to deduce the consequences of Eq. 23 for time-independent fracture description, using a comparison of the fracture growth rate as the basis for similitude at various temperatures.

The choice of the reference temperature in Eq. 22 is of course arbitrary. If we choose temperature T as the reference temperature, then according to Eq. 22, the crack growth rate at temperature T is simply expressed as:

$$\dot{a} = v_c(G/G_f)^{n/2} \tag{23}$$

because $1/T_0 - 1/T = 0$ in this case.

As a basic condition of similitude of fracture at different temperatues, we must now require that the crack growth rate at temperature T must be the same whether expressed on the basis of reference temperature T_0, or reference temperature T. Thus, equating the expressions in Eqs. 23 and 22, we obtain the following approximate formula:

$$G_f = G_f^0 \exp\left(\frac{\gamma}{T} - \frac{\gamma}{T_0}\right) \tag{24}$$

in which

$$\gamma = 2U/nR \tag{25}$$

γ is a constant characterizing the given material.

Eq. 24 may be simply transformed to a linear plot of $\ln G_f$ versus T^{-1}, and linear regression in this plot then yields G_f^0 as well as γ. However, the activation energy values U cannot be determined unless constant n is obtained separately.

Extensive experiments aimed at determining the effect of temperature as well as humidity on the fracture energy of concrete have recently been conducted at Northwestern University by Prat [19]. Fracture energies were obtained for different temperatures according to the size effect (Eq. 5), and it was checked that different types of specimens yield at various temperatures about the same fracture energy values. The dependence of the fracture energy on temperature was found to closely agree with Eq. 24 for both dried concrete and concrete with the saturation water content. The test results obtained by Prat [19] are exhibited in Fig. 3; for a detailed description of the tests and their analysis, see Ref. 19.

CONCLUSION

The size effect, the salient property of fracture mechanics, represents for brittle heterogeneous material such as concrete a smooth transition between failures governed by the strength or yield limit and failures governed purely by fracture energy. This transition is describable by a relatively simple size effect law, which has proven useful as an improvement for various design formulas for concrete structures (diagonal shear in beams, punching shear in slabs, torsional failure of beams, ring and beam failures of pipes, etc.) as well as for the determination of nonlinear fracture parameters of the material, especially the fracture energy. The simple formula represented Bazant's size effect law is also applicable in three dimensions provided that structures that are geometrically similar in three dimensions are considered. A different type of similitude, based on the notion of equivalent crack growth rates, may be exploited to determine the dependence of fracture energy on temperature in the context of time-independent fracture mechanics theory

ACKNOWLEDGMENT. – Partial financial support under U. S. Air Force Office of Scientific Research Contract no. F49620-87-C-0030DEF with Northwestern University, monitored by Dr. Spencer T. Wu, is gratefully acknowledged. Furthermore, thanks for valuable assistance in the study of the temperature effect are due to graduate research assistsant P. C. Prat, and for stimulating discussions on the three-dimensional size effect to doctoral student M. Kazemi.

REFERENCES

1. Bažant, Z. P., "Size Effect in Blunt Fracture: Concrete, Rock, Metal," J. Engrg. Mech., ASCE Vol. 110 1984, 518-535.

2. Bažant, Z. P., "Fracture Mechanics and Strain-Softening of Concrete," in Proceedings, U. S. - Japan Seminar on Finite Element Analysis of Reinforced Concrete Structure, held in Tokyo in May 1985, publ. by ASCE, New York, 1986, pp. 121-150.

3. Bažant, Z. P., "Comment on Hillerborg's Comparison of Size Effect Law with Fictitions Crack Model," in Dei Poli Anniversary Volume, L. Cedolin, Ed., Politecnico di Milano, Milano, 1985, pp. 335-338.

4. Hillerborg, A., "A Comparison Between the Size Effect Law and the Fictitious Crack Model", ibid., pp. 331-334.

5. Bažant, Z. P., and Kim, J. K., Discussion Closure to "Size Effect in Shear Failure of Longitudinally Reinforced Beams," Am. Concrete Institute Journal, Vol. 81, July-August 1985, pp. 580-538.

6. Petch, N. J., "The Cleavage Strength of Polycrystals," Journal, Iron and Steel Institute, Vol. 173, 1953, pp. 25-28.

7. Tetelman, A. S., and McEvily, A. J., "Fracture of Structural Materials," J. Wiley, New York, 1967, p. 186.

8. Cottrell, A. H. "The Mechanical Properties of Matter," J. Wiley, New York, 1964, p. 282.

9. Bažant, Z. P., and Cao, Z., "Size Effect in Punching Shear Failure of Slabs," ACI Materials Journal, Vol. 84, No. 1, Jan.-Feb. 1987.

10. Bažant, Z. P., Sener, S., and Prat, P. C., "Size Effect Tests of Torsional Failure of Concrete Beams," Report No. 86-12/428s, Center for Concrete and Geomaterials, Northwestern University, Evanston, Illinois, Dec. 1986.

11. Tetelman, A. S., and McEvily, A. J., "Fracture of Structural Materials," John Wiley & Sons, New York, 1967, pp. 274-276.

12. Kanninen, M. F., and Popelar, C. H., "Advanced Fracture Mechanics," Oxford University Press, New York, 1985, pp. 17-18, 26-30.

13. Cherepanov, G. P., "Mechanics of Brittle Fracture," MacGraw Hill, 1979, pp. 174, 455 (translated from Russian original published by Nauka, Moscow, 1974).

14. Cottrell, A. H., "The Mechanical Properties of Matter," John Wiley & Sons, New York, 1964.

15. Evans, A. G., and Fu, Y., "The Mechanical Behavior of Alumina," in Fracture in Engineering Materials, ed. by A. G. Evans, Noyes Publications, Park Ridge, N. J., 1984, p. 71.

16. Thouless, M. D., Hsueh, C. H., and Evans, A. G., "A Damage Model of Creep Crack Growth in Polycrystals," Acta Metalurgica, Vol. 31, No. 10, 1983, pp. 1675-1687.

17. Knott, J. F., Fundamentals of Fracture Mechanics, Butterworths, London, England, 1973.

18. Broek, D., "Elementary Engineering Fracture Mechanics," Noordoff International Publishing, Leyden, Netherlands, 1974.

19. Bažant, Z. P., and Prat, P. C., "Effects of Temperature and Humidity on Fracture Energy of Concrete, Report No. 86-12/692e, Center for Concrete and Geomaterials, Northwestern University, Evanston, Illinois, Dec. 1986.

20. Bažant, Z. P., "Mechanics of Distributed Cracking," ASME Applied Mechanics Reviews, Vol. 39, No. 5, May 1986, pp. 675-705.

21. Bažant, Z. P., "Crack Band Model for Fracture of Geomaterials," Proc. 4th Intern. Conf. on Numer. Meth. in Geomechanics, held in Edmonton, Alberta, ed. by Z. Eisenstein, University of Alberta, 1982, Vol. 3, pp. 1137-1152.

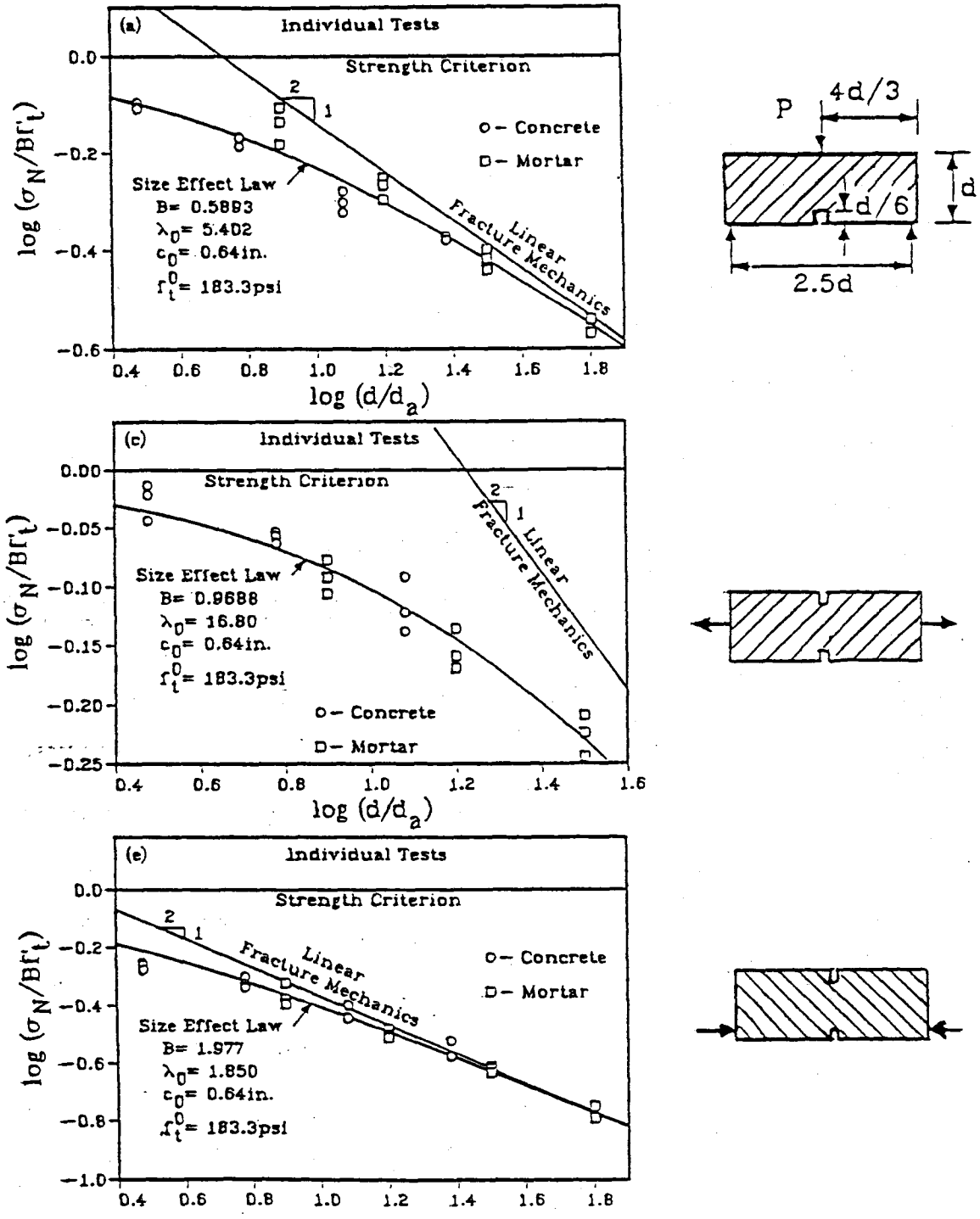

Fig. 1. Nominal stresses at failure vs. specimen size as measured by Bazant and Pfeiffer (1986), and ifts by size effect law.

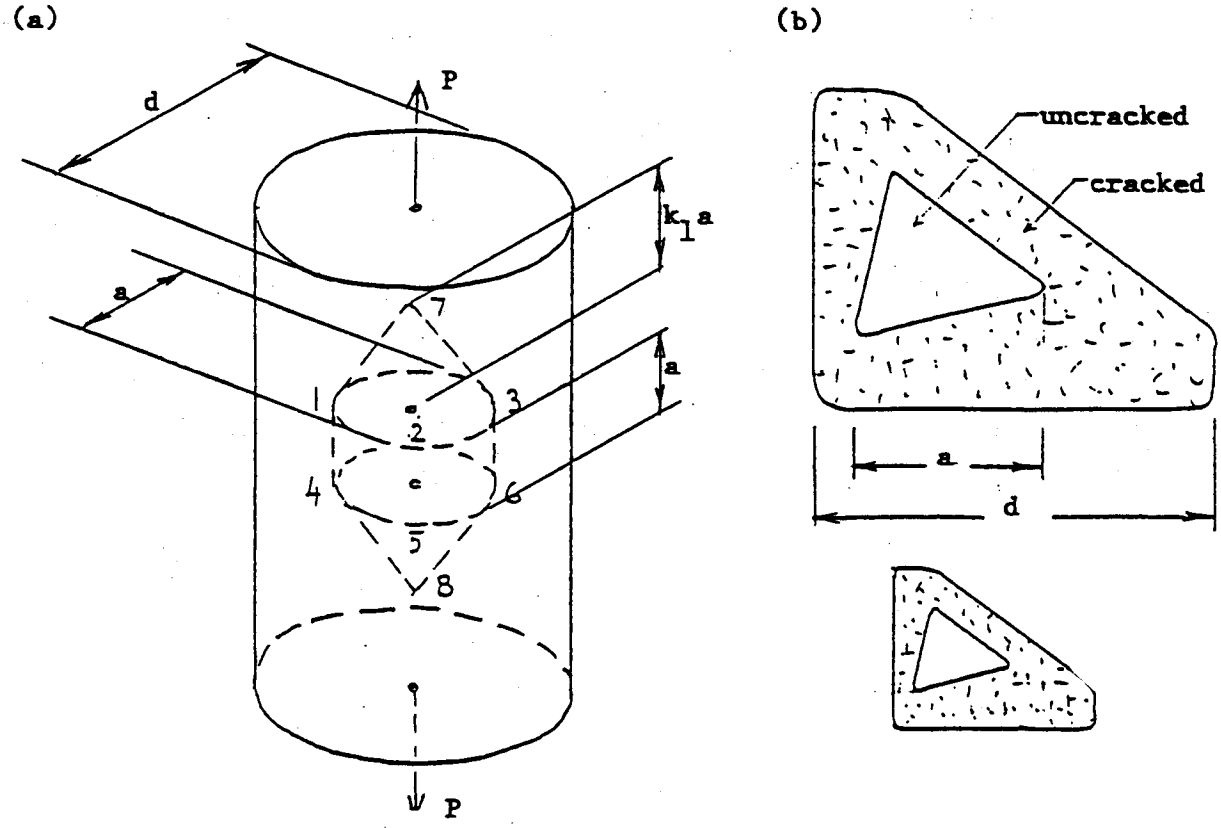

Fig. 2. Three-Dimensional Fracture and its Geometrical Similarity

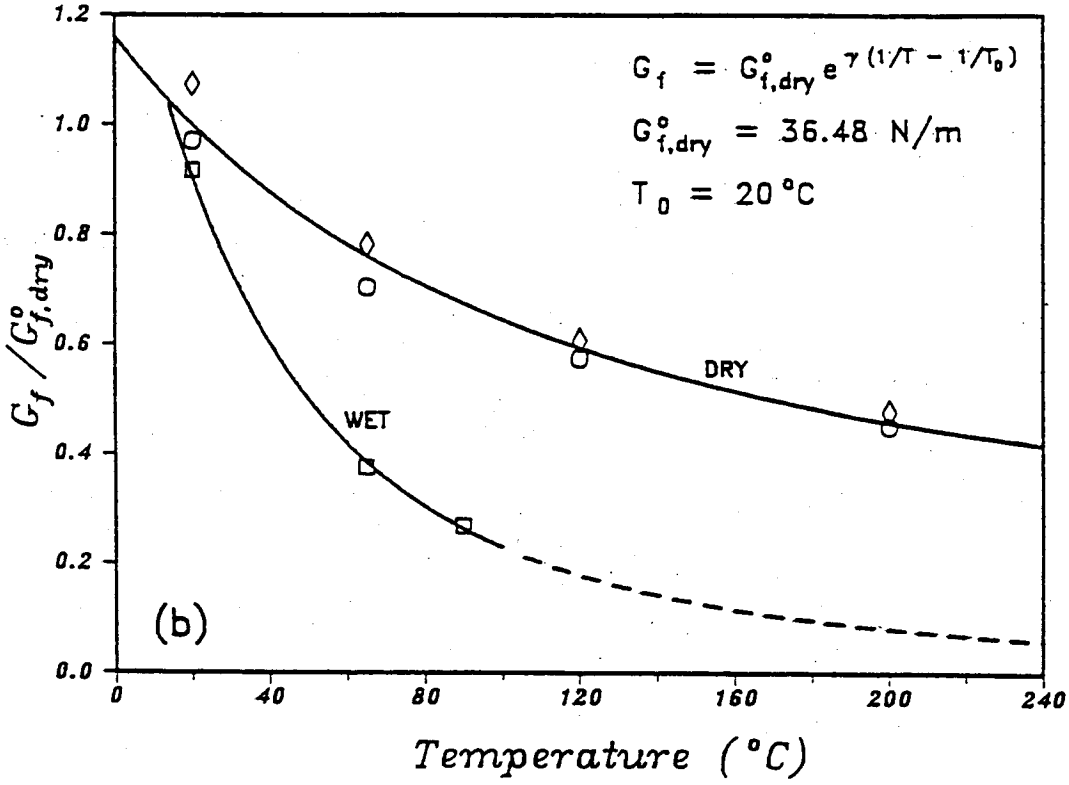

Fig. 3. Test Results of Prat and Bazant (1986) on Temperature Dependence of Fracture Energy of Dry and Wet Concrete

Appendix I. - Deviations from Size Effect Law and Other Size Effects

Transition to Yielding

The similitude of brittle fracture as described by the size effect law may be either limited or entirely overridden by plastic energy dissipation which can occur in plain concrete if there is high confining pressure. E.g., consider the split-cylinder brazilian test on a cylinder of diameter d and thickness (length) b. The formation of the splitting fracture is a brittle event, and so the corresponding load P_f and nominal stress $\sigma_N = \sigma_N^f = P_f/bd$ approximately follows the size effect law. The splitting fracture, however, does not represent a complete failure because a wedge-shaped zone under the load (Fig. 4) must subsequently also slip in order to obtain complete failure. Let the limit load for shearing the wedge off be P_y. If the cylinder is not thin but long, the slip failure of the wedge is essentially plastic since it occurs at high confining pressure (this would not be true for a thin cylinder in which the normal stress in the direction of cylinder axis is small). So the normal stress $\sigma_N^y = P_y/bd$ must be essentially size-independent.

For small enough sizes d we have $P_b > P_y$. Then the maximum load is governed by the size effect law and the plastic wedge shear-off occurs later under a smaller load. However, for a certain sufficiently large size d_{max}, σ_N^f becomes smaller than σ_N^y, and then the load must further increase after the formation of the splitting fracture until it reaches maximum P_y when the wedge shears off plastically. For this type of behavior the size effect plot has the shape shown in Fig. 4b, given as

$$\sigma_N = \sigma_N^f = Bf_t' \left(1 + \frac{d}{\lambda_0 d_a}\right)^{-1/2} \text{ if } \sigma_N > \sigma_N^y \qquad (26)$$

Otherwise $\sigma_N = \sigma_N^y$

The size effect in the brasilian test was recently measured by T. Shioya and T. Hasegawa at Shimizu Institute of Technology, Tokyo (private communication in May 1985 and Jan. 1987). Their results appear to agree with the behavior shown in Fig. 4b, although there is inevitably considerable random scatter in this kind of test. It may be noted that if the specimens for all the sizes were thin and had the same thickness, sufficient confining pressure could not develop to permit plastic failure of the wedge, and then σ_N^y would be negligibly small. It should also be noted that when the large specimens are much thicker than the small ones, they can heat up significantly due to hydration, and this effect as well as the effect of heating on moisture loss can then superimpose a different size effect.

A different type of yielding effect may apparently be obtained when the yielding occurs simultaneously with the propagation of the cracking zone (fracture) at maximum load. This is apparently the case for the diagonal shear ailure of beams with stirrups. As shown in Ref. 1, the size effect for this type of yielding effect should follow the equation:

$$\sigma_N = Bf_t' \left(1 + \frac{d}{\lambda_0 d_a}\right)^{1/2} + \sigma_y \qquad (27)$$

as one can show by analyzing the energy balance at failure.

Other Types of Size Effect

Three types of size effects can be distinguished in concrete structures:

1. Fracture mechanics size effect, due to fracture propagation and energy release.
2. Diffusion-type size effect due to heat conduction and water diffusion.
3. Statistical size effect due to randomness of material properties.

The size effects due to heat condition and water diffusion play a major role in creep and shrinkage but they can also interfere with the size effect law for blunt fracture. Particularly when specimens that are geometrically similar in three rather than two dimensions are compared, the large specimens may heat up significantly due to hydration, which accelerates the hardening of concrete. This then leads to higher f_t' as well as G_f, thus altering the parameters of Eq. 1. At the same time, the heating may produce thermal stresses which cause cracking or at least tensile strain-softening. This may then reduce the effective strength and fracture energy for externally applied load. Drying arrests hydration, and, therefore, a smaller specimen has a smaller gain in strength and in fracture energy than a larger specimen over the same period of time. But in a larger specimen, nonuniform drying may cause more cracking or tensile strain-softening, which could cause an opposite tendency. The diffusion type size effects may be described by simple formulas only in some simple situations (e.g., in the BP Model for shrinkage and drying creep). Generally they defy description by a simple law and call for complete stress and cracking analysis.

Statistical Size Effect

The statistical size effect in failure is described by Weibull theory. This theory is applicable to the failure of a chain of brittle elements. It predicts the strength of the chain to decrease as the length of the chain is increased, because the chance of encountering a lower strength in a longer chain increases as the length of the chain increases. Thus, e.g., Weibull theory no doubt applies to the length effect in tensile failure of a long and thin uniaxially stressed concrete bar without notches.

However, for failures that occur after a large crack has already developed, which is the majority of failures in concrete structures, the Weibull-type statistical effect plays probably an insignificant role. The reason is that the zone in which the fracture front at failure can be located is, due to the mechanics of failure, rather small compared to the volume of the structure, even if the structure is rather large.

The Weibull distribution of strength R is defined as $F(R) = 1 - \exp[-k_1 V(R-R_0)^{\alpha}]$ where V = volume of the structure, and R_0, k_1, α = constants, R_0 = minimum strength. The mean of R is the tensile strength f'_t. It can be shown that the statistical aspect of fracture would cause in the size effect law (Eq. 1) a modification of f'_t. With the inclusion of the effect of d_a (Eq. 4), this modification may be written as follows:

$$\sigma_N = \frac{B}{\sqrt{1 + \frac{d}{\lambda_0 d_a}}} \left[R_0 + c\left(\frac{V_{fr}}{V}\right)^{1/\alpha} \left(\frac{d}{d_a}\right)^{-2/\alpha}\right] \qquad (28)$$

V_{fr} is the volume of the zone in which the mechanics of failure permits the crack front a the moment of failure to be possibly located (Fig. 5), and V = total volume of the specimen.

Now, an important point is that, for brittle structural failures with fairly reproducible failure modes, such as the diagonal shear failure of beams, the volume V_{fr} is very small compared to V. This means that the effect of statistical variation of strength must be much smaller than it is for a long bar in tension. If the material parameters R_0, k, and α are calibrated to give a reasonable statistical size effect for a long thin concrete bar in tension, the use of the same material parameters for structural failures such as the diagonal shear failure given in Eq. 27 yields only a very small correction, because the ratio V_{fr}/V is rather small. It is for this reason that the statistical size effect in diagonal shear failure appears to be unimportant.

Derivation of Eq. 5

For $d \to \infty$, the size effect law (Eq. 1) yields:

$$\sigma_N = B\, t\, (\lambda_0\, a)^{2} \qquad (29)$$

This must be equivalent to linear elastic fracture mechanics, which yields for all structure geometries:

$$\sigma_N = [G_f E / g(\alpha_0)]^{1/2}\, d^{-1/2} \qquad (30)$$

Eqs. 29 and 30 must be equivalent, and equating them one gets the last expression in Eq. 5. A slightly different derivation was originally given on p. 293 in Bažant, Kim and Pfeiffer (1986, J. of Str. Eng. ASCE 112).

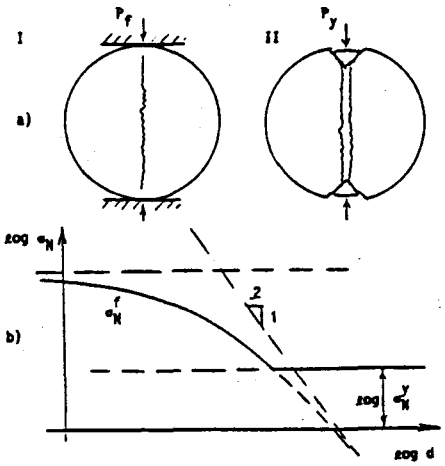

Fig. 4 Brittle Failure with Yielding (a), and the corresponding size effect (b).

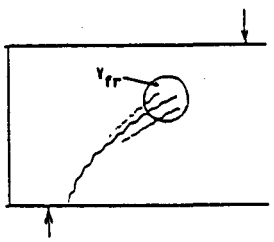

Fig. 5 Volume V_{fr} in which crack front can be located (due to random scatter of material properties).

Appendix II. - Brittleness Number

The fact that the size effect law yields approximately the same fracture energy values regardless of specimen size and shape makes it possible to base on the size effect law a nondimensional characteristic for the type of fracture behavior, which we may call the brittleness number. It may be defined as

$$\beta = \frac{d}{\lambda_0 \, d_a} \tag{31}$$

and can be calculated after λ_0 has been determined either experimentally or by finite element analysis. The value $\beta = 1$ indicates the value of d/d_a at the point where the horizontal asymptote for the strength criterion intersects the inclined straight-line asymptote for linear elastic fracture mechanics (Fig. 1). So, β represents the center of the transition between these two extreme types of fracture behavior. For $\beta > 1$, the behavior is closer to plastic limit analysis, and for $\beta < 1$ it is closer to linear elastic fracture mechanics. For $\beta < 0.1$, the plastic limit analysis may be used as an approximation, and for $\beta > 10$, linear elastic fracture mechanics may be used as an approximation. For $0.1 < \beta < 10$, nonlinear fracture analysis must be used. The brittleness number can serve as a basic qualitative indicator of the type of fracture response, and in this sense it is in fact analogous to the nondimensional characteristics used, e.g., in fluid mechanics, such as the Reynolds number.

A. Carpinteri (Engng. Fract. Mech. 16, 1982, p. 467-481) previously proposed to characterize the efect of the structure size on its brittleness by the ratio $s = G_f/b\,f_t'$. A. Hillerborg (Mat. Str., RILEM, 18, 1985, pp. 25-30) characterized the effect of size on structure brittleness by the ratio of the structure size to the characteristic length defined as $\ell_{ch} = E_c G_f/f_t'^2$. The use of these characteristics is, however, limited, since they can correlate only specimens or structures of the same geometry. They have the disadvantage that for the same value of this brittleness characteristic, a specimen of one shape may be quite brittle (i.e., close to linear elastic fracture mechanics), while a specimen of another shape may be quite ductile (i.e., close to plastic limit analysis). The brittleness number defined by Eq. 31 is free of this limitation, making it possible to compare in brittleness a small structure of one shape with a large structure of another shape. The greater generality of β is due to the fact that it is related not only to G_f, E_c and f_t' (through Eq. 1) but also to the size (width or length) of the fracture process zone (see Ref. 7) which is independent of the aforementioned characteristic length ℓ_{ch}, and also to geometry of the structure.

The change of load-deflection response of a structure of a certain geometry as a function of β is illustrated in Fig. 6. An increase in structure size causes that a further elastic deformation (Fig. 6b) is superimposed on the original deformation for small size at the same load P (Fig. 6a). This means that the displacements A and B or A and D in Fig. 6a and b or 6a and d (lines I and II) must be added. The resulting response diagrams are shown in Fig. 6c for the case that the additional elastic deformation is of medium value, or large. It is clear that for a sufficiently large structure the resulting load-deflection diagram must exhibit snap-back, and when this structure is loaded in a displacement-controlled manner this must then lead to snap-down instability represented by the dynamic passage from point 2 to point 4 in Fig. 6e, in which the structure acquires the kinetic energy indicated by the cross-hatched area which is ultimately dissipated as heat. This graphical construction clearly illustrates that a sufficient increase of size must lead to purely brittle, i.e., dynamic, explosive failure.

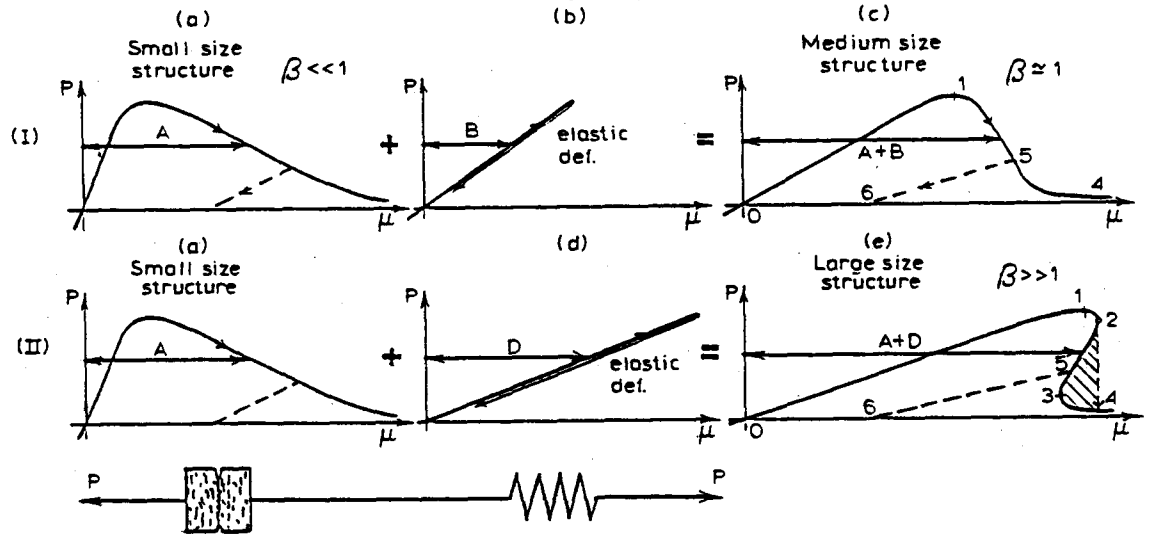

Fig. 6 - Explanation of the Effect of the Size on Brittleness